

## Novel SiC detector based on optical signal instead of electrical signal

Geunsik Lim,<sup>1</sup> Tariq Manzur,<sup>2</sup> and Aravinda Kar<sup>1</sup>

<sup>1</sup>CREOL, The College of Optics and Photonics,  
Laser-Advanced Materials Processing Laboratory, Departments of MAE and MSE,  
University of Central Florida, Orlando, Florida 32816-2700, U.S.A.

<sup>2</sup>S&T Lead, I&EW, Undersea Warfare Electromagnetic Systems Development, Building 1319,  
1176 Howell Street, Newport, RI 02841-1708, U.S.A.

### ABSTRACT

A novel SiC optical detector that produces optical signal in contrast to the electric signal generated by conventional electrical detectors. The optical detector is a remote sensor providing response to incident photons from a distant object. The incident photons modify the refractive index and, consequently, the reflectance of the doped SiC by altering the electron densities in the valence band and the acceptor energy levels. This variation in the refractive index or reflectance represents the optical signal as the sensor response, which can be determined with a probe laser such as a He-Ne laser or a light-emitting diode. The sensor can be applied to numerous remote sensing applications including high-temperature or harsh environments due to the optical read-out of the detector response with a probe laser. The effects of different dopants on the detector response for sensing different chemical species, or equivalently imaging in different MWIR wavelengths, have been studied and the dopant concentration has been found to affect the optical signal. These results indicate that a new class of SiC detectors classified as optical detectors can be produced for a variety of wavelengths using different dopants for numerous applications.

### INTRODUCTION

Crystalline silicon carbide (SiC) is chemically inert and it has high electric breakdown strength, thermal conductivity and mechanical strength, which make it an excellent material for numerous high-temperature applications including high-voltage and high-current devices, and sensors for harsh environments. Different SiC device architectures such as capacitors, transistors and Schottky diodes have been studied as potential gas sensors. Andersson et al. [1] developed a new generation SiC field effect transistor (FET) for gas sensing applications, and Darmastuti et al. [2] and Bur et al. [3] employed the SiC FET for detection of methanol leakage and quantification of NO<sub>x</sub>, respectively. Zhang et al. [4] studied boron-doped carbon nanotubes for sensing HCN, and Wu et al. [5] examined SiC nanotubes as gas sensors for CO and HCN.

The conventional chemical sensors generally measure the changes in electrical properties, such as resistance or capacitance, of a thin film that is in contact with the chemical of interest. Optical gas sensors, on the other hand, rely on the modifications in optical properties, such as refractive index, by the characteristic radiation emitted by the chemical of interest. Optical gas sensors can operate remotely with significant stand-off from the source of the chemical, possess rapid response time for dynamic environments and enable measuring very low gas concentrations. The remote sensing capability makes optical sensors suitable for harsh environment applications. These sensors have been demonstrated to be highly sensitive to several gases [6-8]. The temperature, pressure and chemical sensing capability of single crystal

SiC substrates has been studied [9-11] using optically reflective and interferometric techniques. Chakravarty et al. [11] examined this type of sensors at high pressures (up to 600 psi) and high temperatures (up to 500°C), and showed that no external interferometer is necessary because SiC acts inherently as a Fabry-Pérot interferometer. Lim and Kar [12, 13] introduced the concept chemical sensing with SiC utilizing the change in the refractive index by the characteristic radiation of the chemical, and measuring the subsequent change in the reflectance of SiC.

### Operating principle of the optical sensor

The principle of the SiC optical sensor is that the characteristic photons emitted by the chemical of interest excite electrons from the valence band to an acceptor energy level as shown in figure 1. SiC is doped with an appropriate dopant that creates an energy level ( $E$ ) corresponding to the wavelength ( $\lambda$ ) of the characteristic radiation emitted by the gas, so that  $E=hc/\lambda$ , where  $h$  and  $c$  are Planck's constant and the speed of light, respectively. The photoexcitation process changes the electron density in the valence band and the acceptor energy level and, therefore, affects the refractive index. Consequently, the reflectance of the doped SiC is modified. The refractive index can be probed with a laser beam, such as a He-Ne laser, by measuring the reflected power. The changes in the refractive index or reflectance can be used as the sensor response.

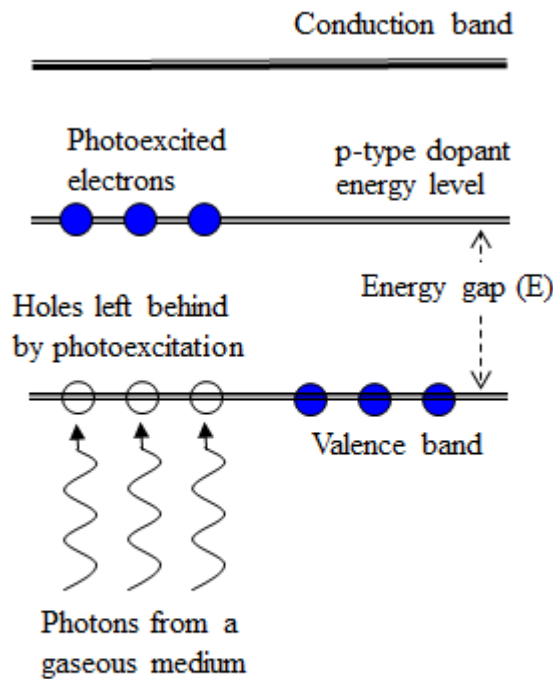


Figure 1. Modification of electron density in the valence band and acceptor energy level due to electronic transition by photoexcitation.

NO, CO<sub>2</sub>, CO and NO<sub>2</sub> gases yield the characteristic wavelengths of these gases as 5.26, 4.30, 2.35 and 6.25  $\mu\text{m}$  corresponding to a single photon energy of 0.23, 0.28, 0.52 and 0.19 eV, respectively [15-17]. These dopants can, therefore, be utilized to fabricate optical sensors for these gases.

Dopant selection is a critical step for fabricating the sensor to detect a given chemical. Generally, the acceptor energy level of a particular dopant element in a semiconductor can be determined by the density functional theory. Experiments, however, can also be carried out to determine the energy levels for different dopants. Lebedev [14] reported a set of dopant elements and their energy levels, indicating that Al, Ga and Sc atoms produce energy levels 0.23, 0.29 and 0.52 eV, respectively, above the valence band maximum of 6H-SiC, and P produces an energy level 0.14 eV below the conduction band minimum. The spectroscopic data of

## EXPERIMENTAL PROCEDURE

### Laser doping for sensor fabrication

In the laser doping process, the substrate, which is SiC in this case, is placed in a vacuum doping chamber (figure 2). After creating a suitable vacuum, the chamber is filled with a dopant precursor such as a metallorganic compound. When the substrate is heated with a laser beam, the precursor undergoes chemical decomposition at the laser-heated spot, producing the dopant atoms that subsequently diffuse into the substrate. Triethylgallium (TMG),  $(C_2H_5)_3Ga$ , can be used as a precursor for doping 6H-SiC with Ga to fabricate a  $CO_2$  gas sensor. For this purpose, an n-type 6H-SiC square substrate of side 1 cm and thickness 279  $\mu m$  was cleaned in a solution of  $H_2O_2:H_2SO_4$  (1:1 by volume) for 15 minutes. The sample was further cleansed with deionized (DI) water and buffered oxide etching solution. This clean sample was placed in a vacuum ( $\sim 1$  mTorr) doping chamber and the precursor TMG was supplied to the chamber from a bubbler using an inert gas, e.g., argon as shown in figure 2. The bubbler was kept at a constant temperature of 100°C. The SiC substrate was then heated with a continuous wave (CW) Nd:YAG ( $\lambda = 1.064$   $\mu m$ ) laser beam. The doping process parameters were: laser

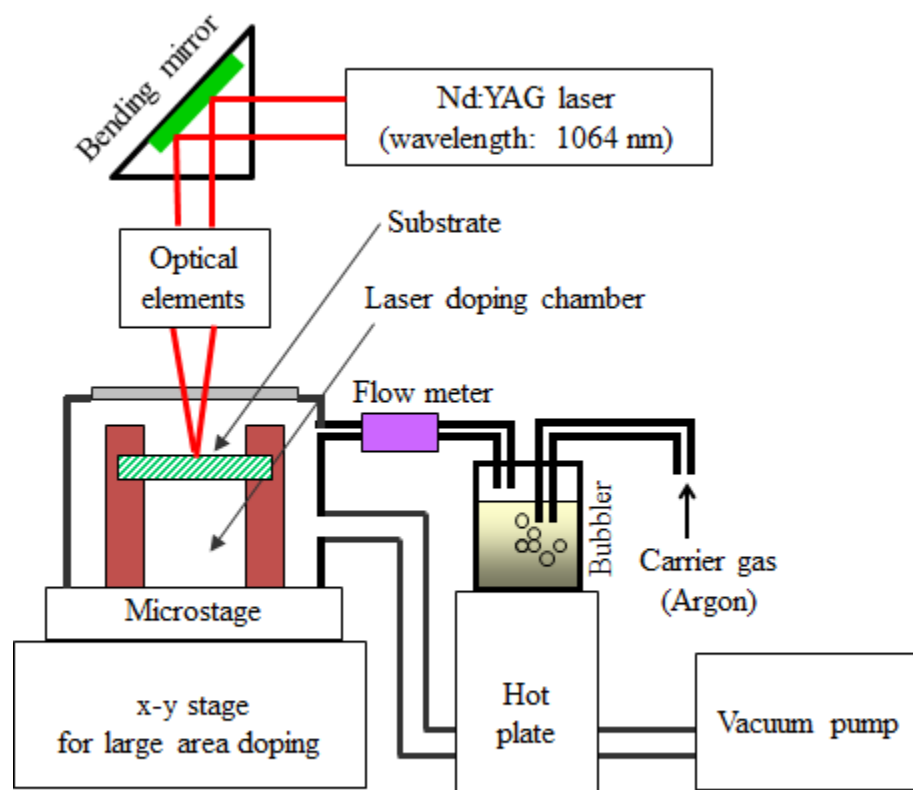


Figure 2. Experimental setup for a laser doping system.

power = 10.5 W, focal length of the lens = 150 mm, laser beam diameter = 200  $\mu m$  and scanning speed = 0.8 mm/s. Ga atoms, which are produced due to thermal decomposition of TMG at the laser-heated spot, diffuse into the substrate to create a doped region. After creating a doped line, the substrate was moved in the lateral direction with an x-y stage to create another doped line contiguous to the previous line. This process was continued to dope the substrate over a large area. The doped sample was cleaned with a 45 wt.% KOH solution and rinsed with acetone, methanol and DI water for testing the sensor response.

of  $H_2O_2:H_2SO_4$  (1:1 by volume) for 15 minutes. The sample was further cleansed with deionized (DI) water and buffered oxide etching solution. This clean sample was placed in a vacuum ( $\sim 1$  mTorr) doping chamber and the precursor TMG was supplied to the chamber from a bubbler using an inert gas, e.g., argon as shown in figure 2. The bubbler was kept at a constant temperature of 100°C. The SiC substrate was then heated with a continuous wave (CW) Nd:YAG ( $\lambda = 1.064$   $\mu m$ ) laser beam. The doping process parameters were: laser

To produce multiple gas sensors in a single substrate, the above-mentioned Ga-doping was carried out in one of the four quadrants of the substrate for sensing CO<sub>2</sub> gas. The other three quadrants were doped with Al, Sc and P to produce sensors for NO, CO and NO<sub>2</sub> gases, respectively, as shown in figure 3. The precursors for Al, Sc and P dopants were trimethylaluminum [TMA: CH<sub>3</sub>)<sub>3</sub>Al], a solution of the solute Scandium(III) hexafluoroacetylacetonate [Sc(hfac): Sc(C<sub>5</sub>HF<sub>6</sub>O<sub>2</sub>)<sub>3</sub>] in the solvent dimethyl sulfoxide [DMSO: (CH<sub>3</sub>)<sub>2</sub>SO], and Trimethylphosphine [TMP: CH<sub>3</sub>)<sub>3</sub>P], respectively.

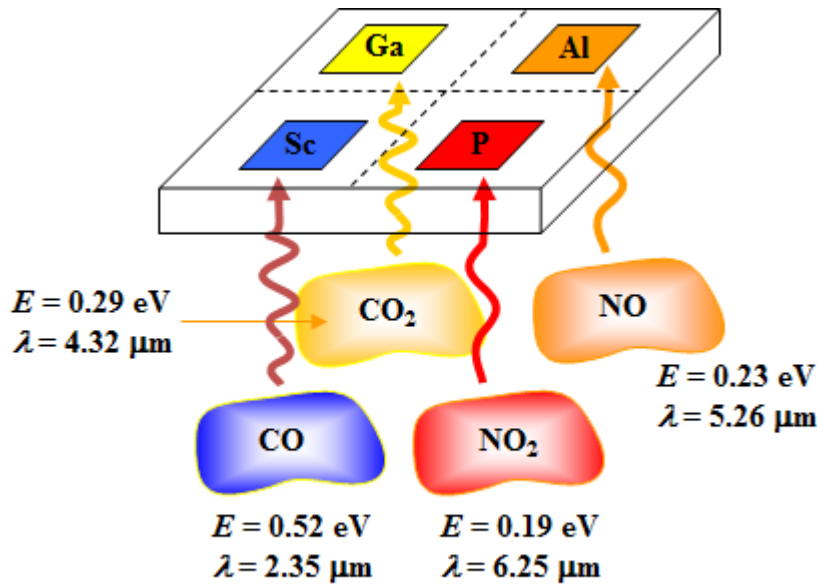


Figure 3. Multiple gas sensors on a single substrate.

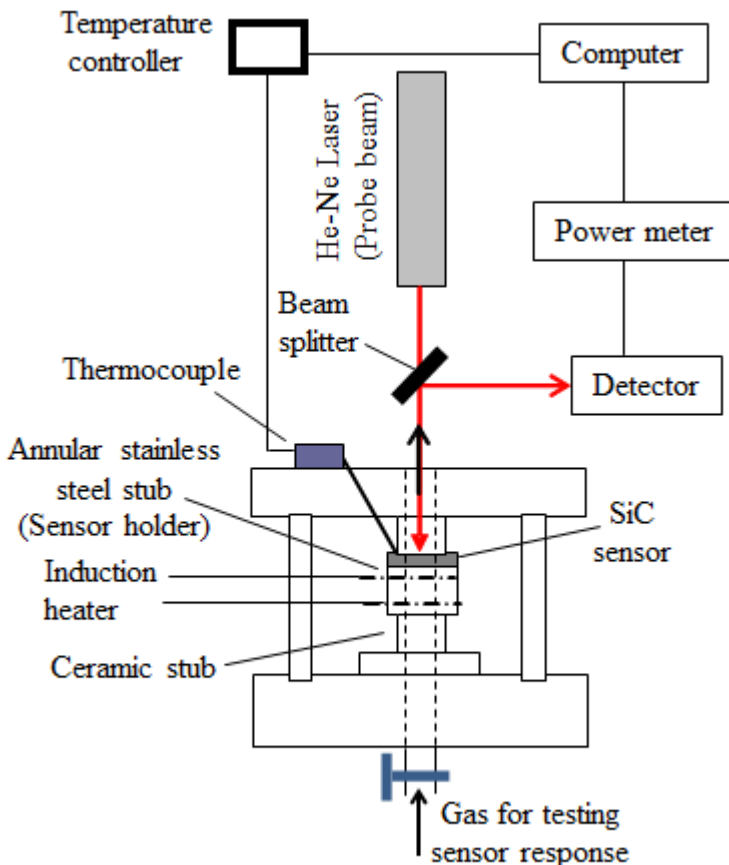


Figure 4. Apparatus for Sensor response measurement.

### Testing of sensor response

The sensor response, which is indicated by the changes in the reflected power of a probe beam, is measured using an apparatus shown in figure 4. The doped sample was placed on a sensor holder, which was an annular cylindrical stub made of stainless steel. The gas, for which the sensor response was to be measured, was supplied to the annular space from a gas cylinder and the gas was heated by inductively heating the sample holder. This high temperature testing simulates the sensor response for combustion gases since the intensity of radiation increases with temperature. A continuous wave He-Ne laser (wavelength 632.8 nm) of power 15 mW was directed to the sensor (doped region) at normal incidence through a beam splitter. The laser beam, which was reflected off the sensor, was directed to a

photodetector by the beam splitter and the reflected power was measured with a power meter. The variation in the reflected power as a function of the gas temperature was stored in a computer. One of the important optical properties of doped SiC is that it inherently acts as a Fabry-Pérot interferometer in which the laser beam reflects off both the top and bottom inner surfaces of the sensor. Such reflections create a multibeam interference pattern, which is analyzed to calculate the change in the refractive index of the sensor for a given gas.

## RESULTS AND DISCUSSION

The absorption spectra of the doped samples were examined to verify whether the dopants create an energy level to allow absorption of incident photons. Typical results for the as-received, Ga-doped and Al-doped samples are presented in figure 5. The as-received sample exhibits absorbance of ~20% in the wavelength range of 4.32 to 5.26  $\mu\text{m}$ . The Ga-doped sample,

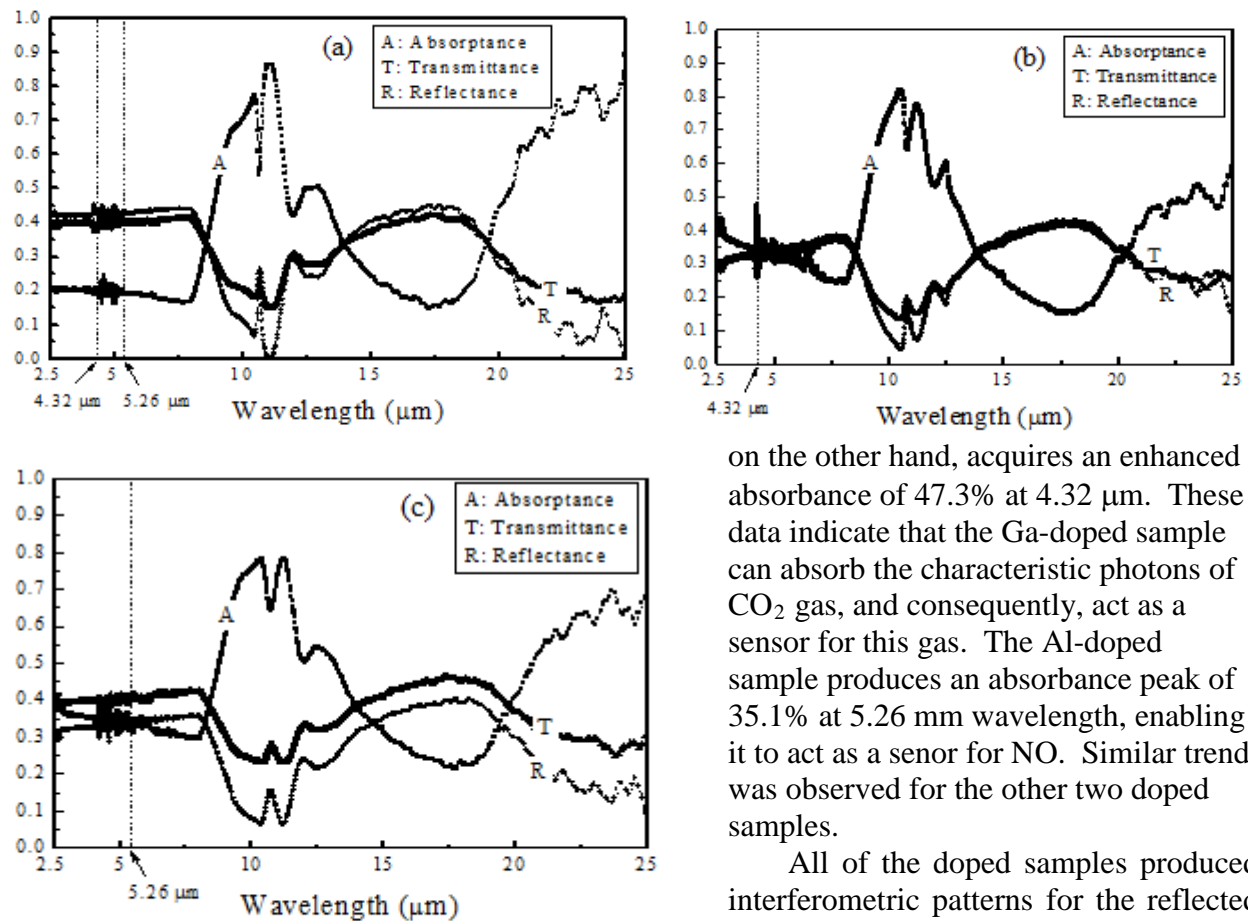


Figure 5. Absorbance of 6H-SiC samples: (a) as-received, (b) Ga-doped and (c) Al-doped, showing enhanced capability of the doped samples for sensing  $\text{CO}_2$  and  $\text{NO}$  gases, respectively.

on the other hand, acquires an enhanced absorbance of 47.3% at 4.32  $\mu\text{m}$ . These data indicate that the Ga-doped sample can absorb the characteristic photons of  $\text{CO}_2$  gas, and consequently, act as a sensor for this gas. The Al-doped sample produces an absorbance peak of 35.1% at 5.26  $\mu\text{m}$  wavelength, enabling it to act as a sensor for  $\text{NO}$ . Similar trend was observed for the other two doped samples.

All of the doped samples produced interferometric patterns for the reflected power of the He-Ne laser for different gases, such as air,  $\text{CO}$ ,  $\text{CO}_2$ ,  $\text{NO}$ , and  $\text{NO}_2$  gases as a function of temperature. The cyclic pattern alternates between certain maximum and minimum values with the change in temperature. The pattern tends to be denser progressively with temperature and the oscillations are unique to the type of the gas, signifying that these patterns can be attributed to the characteristic identity of

the individual gas. The variation in the refractive index can be obtained from this pattern for each gas by considering multibeam interference in the SiC sensors [10].

The interference pattern and the change in the refractive index ( $\Delta n$ ) of Ga-doped 6H-SiC sensor are presented in figures 6a and 6b, respectively. The refractive index of this sample clearly exhibits selectivity for carbon dioxide because  $\Delta n$  varies significantly from a very small value at room temperature to about 0.065 at 650°C. This large value of  $\Delta n$  indicates that the optical sensor would be capable of detecting very small concentration of the gas. The as-received sample also shows very good variation for  $\Delta n$  since the as-received sample had an intrinsic absorbance peak as shown in figure 5a.

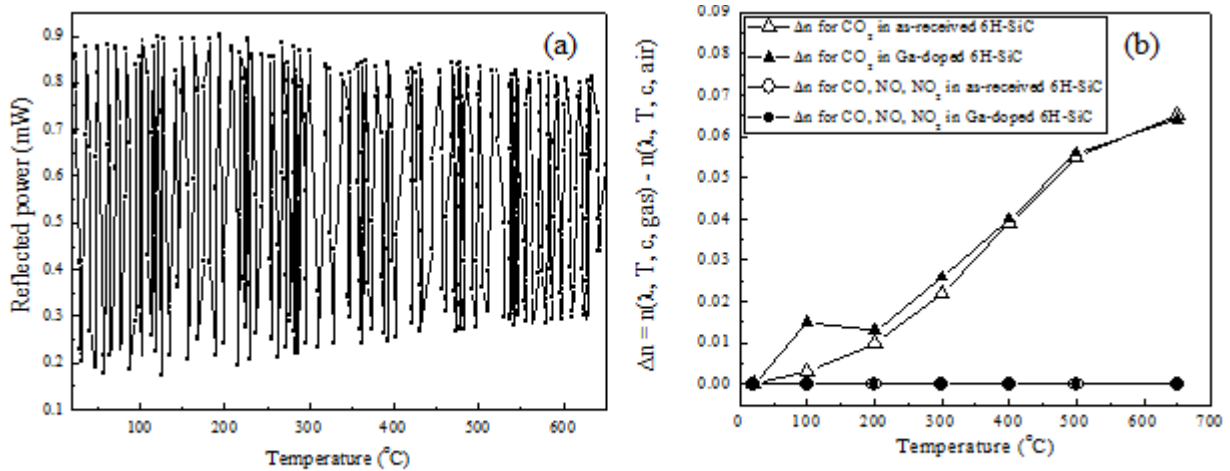


Figure 6. Interference pattern (a) and  $\Delta n$  (b) for Ga-doped 6H-SiC  $\text{CO}_2$  gas sensor.

For Al-doped 6H-SiC NO gas sensor, the interference pattern and  $\Delta n$  are presented in figures 7a and 7b, respectively. The sensor responds strongly to NO gas, indicating special selectivity for this gas with a value of 0.04 at 650°C.

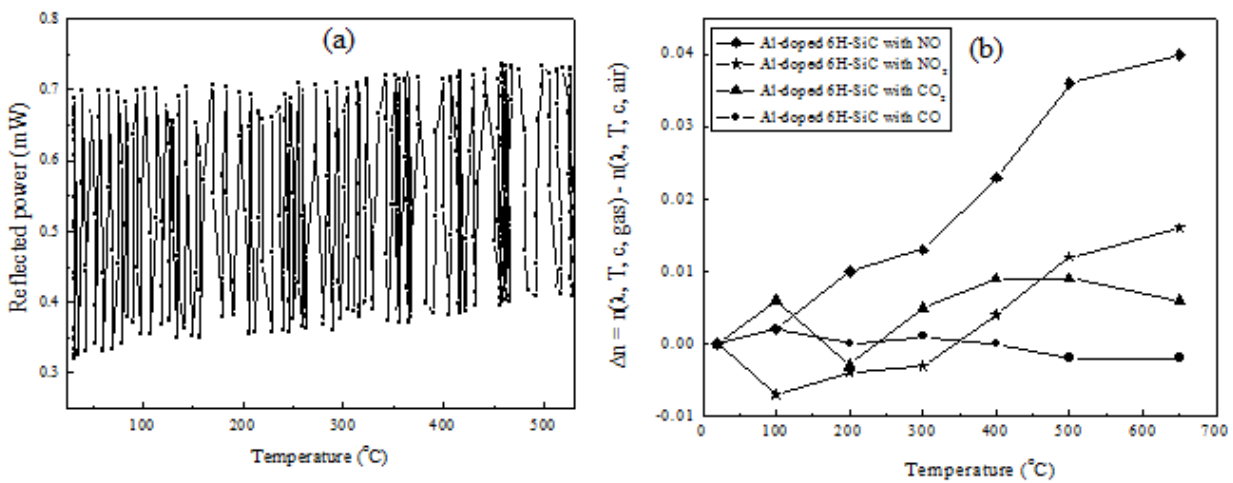


Figure 7. Interference pattern (a) and  $\Delta n$  (b) for Al-doped 6H-SiC NO gas sensor.

For Sc-doped 6H-SiC sensor, the interference pattern and  $\Delta n$  are presented in figures 8a and 8b, respectively. The sensor exhibits distinct selectivity for CO at temperatures higher than 400°C. Also the refractive index varies significantly with a value of 0.05 at 650°C. For P-doped 6H-SiC, the interference pattern and  $\Delta n$  are presented in figures 9a and 9b, respectively. This sensor dominates selectivity for NO<sub>2</sub> gas after about 500°C with a value of  $\Delta n$  0.055 at 650°C. It should be noted that P is an n-type dopant in 6H-SiC, whereas Ga, Al and Sc are p-type dopants. So photoexcitation occurs from the donor energy level to the conduction band in the P-doped sample, and this effect may cause the P-doped sample to be less sensitive at low temperatures. Also the as-received sample was n-type, which may contain multiple donor energy levels, and this characteristic of the starting substrate may be attributed to the low selectivity of the P-doped sensor for NO<sub>2</sub> gas at low temperatures.

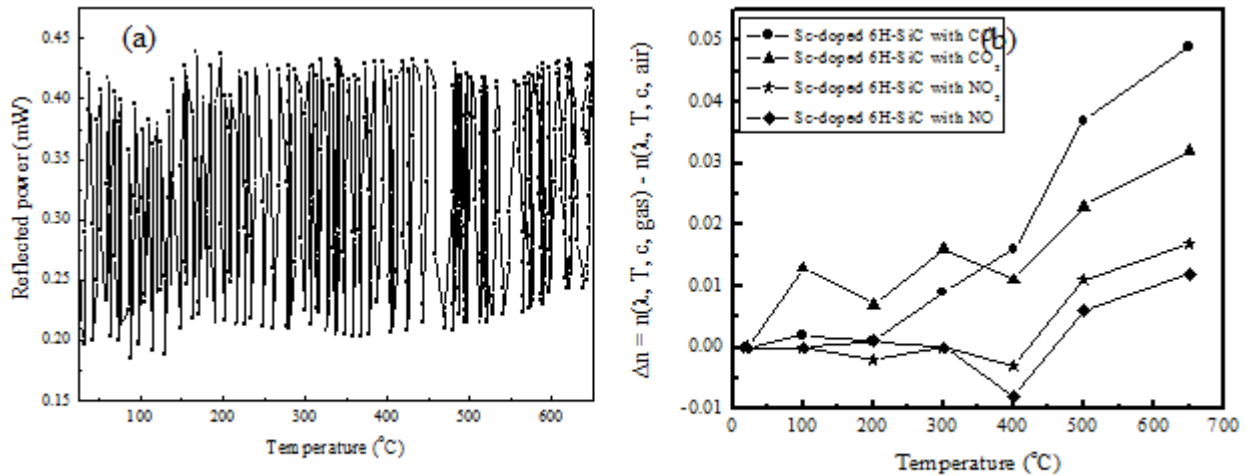


Figure 8. Interference pattern (a) and  $\Delta n$  (b) for Sc-doped 6H-SiC CO gas sensor.

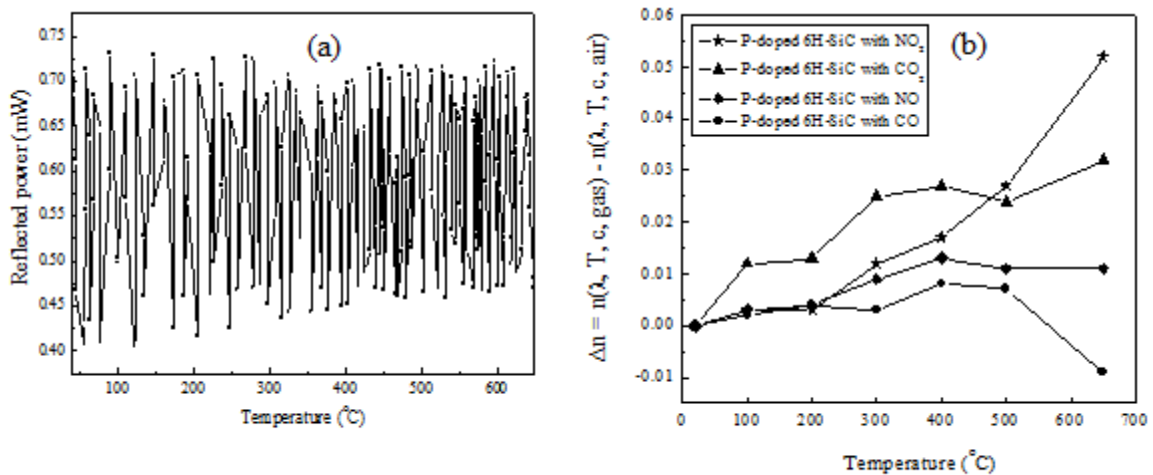


Figure 9. Interference pattern (a) and  $\Delta n$  (b) for P-doped 6H-SiC NO<sub>2</sub> gas sensor.

## CONCLUSION

The utilization of absorption and emission spectra of gases to design and fabricate optical sensors has been demonstrated. A laser doping process can be employed to dope SiC substrates for fabricating the sensors. No post-processing for electrical contacts to the substrate is necessary; the doped sample acts as a sensor by itself. Multiple gas sensors can be built in a single substrate. It is a wireless, remote sensor and its optical signal can be read with a probe laser beam from a long stand-off distance, making it ideal for combustion gas sensing applications. An n-type 6H-SiC substrate has been laser-doped with Ga, Al, Sc and P dopants to produce sensors for various combustion gases, particularly CO<sub>2</sub>, NO, CO and NO<sub>2</sub> gases, respectively. The optical signal, refractive index, changes significantly at high temperatures, indicating that the sensors can be used for detecting small concentrations of gases.

## REFERENCES

1. M. Andersson, R. Pearce and A. L. Spetz, *Sensors and Actuators B: Chemical* **179**, 95 (2013).
2. Z. Darmastuti, P. Bhattacharyya, M. Andersson, J. Kanungo, B. Basu, L. Ojamae, A. L. Spetz, *Sensors and Actuators B: Chemical* **187**, 553 (2013).
3. C. Bur, P. Reimann, M. Andersson, A. Lloyd Spetz, and A. Schütze, *Microsystem Technologies* **18**, 1015 (2012).
4. Y. Zhang, D. Zhang, C. Liu, *J. Phys. Chem.* **B110**, 4671 (2006).
5. R. Wu, M. Yang, Y. Lu, Y. Feng, Z. Huang, Q. Wu, *J. Phys. Chem.* **C112**, 15985 (2008).
6. A. Egorov, M. Egorov, T. Chekhlova, A. Timakin, *Quantum Electron.* **38**, 787 (2008).
7. A. Setaro, A. Bismuto, S. Lettieri, P. Maddalena, E. Comini, S. Bianchi, C. Baratto, G. Sberveglieri, *Sensors and Actuators* **B130**, 391 (2008).
8. H. Nam, T. Sasaki, N. Koshizaki, *J. Phys. Chem.* **B110**, 23081 (2006).
9. S. Dakshinamurthy, N. Quick, A. Kar, *J. Appl. Phys.* **99**, 94902 (2006).
10. S. Dakshinamurthy, N. Quick, A. Kar, *J. Phys. D: Appl. Phys.* **40**, 353 (2007).
11. A. Chakravarty, N. Quick, A. Kar, *J. Appl. Phys.* **102**, 73111 (2007).
12. G. Lim, U. P. DeSilva, N. R. Quick and A. Kar, *Appl. Opt.* **49**, 1563 (2010).
13. G. Lim, T. Manzur and A. Kar, *Appl. Opt.* **50**, 2640 (2011).
14. A. A. Lebedev, *Semiconductors* **33**, 107 (1999).
15. A. J. Castro, J. Meneses, S. Briz, and F. Lopez, *Rev. Sci. Instrum.* **70**, 3156 (1999).
16. U. Willer, M. Saraji, A. Khorsandi, P. Geiser, and W. Schade, *Optics and Lasers Eng.* **44**, 699 (2006).
17. H. Herbin, N. Picque, G. Guelachvili, E. Sorokin, and I. Sorokina, *J. Molecular Spectroscopy*, **238**, 256 (2006).